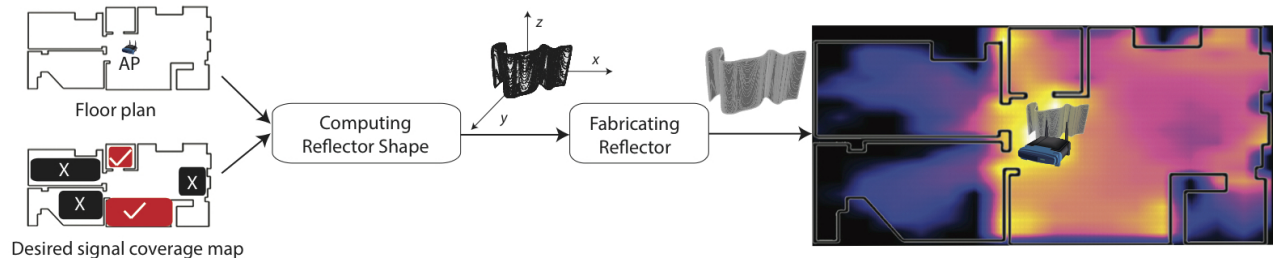


# 3D Printing Your Wireless Coverage

Justin Chan\*, Changxi Zheng†, Xia Zhou\*  
Dartmouth College\*, Columbia University†  
{justin.k.l.chan, xia.zhou}@dartmouth.edu, cxz@cs.columbia.edu



**Figure 1: Overview of WiPrint system.** User can input a floor plan, location of an AP and a desired signal map to the system. The desired signal pattern is marked with red and black regions indicating areas which should have strong and weak signals respectively. WiPrint uses an optimization algorithm to produce a reflector shape. This reflector is then fabricated and applied to an AP to achieve this desired signal pattern.

## ABSTRACT

Directing wireless signals and customizing wireless coverage is of great importance in residential, commercial, and industrial environments. It can improve the wireless reception quality, reduce the energy consumption, and achieve better security and privacy. To this end, we propose WiPrint, a new computational approach to control wireless coverage by mounting signal reflectors in carefully optimized shapes on wireless routers. Leveraging 3D reconstruction, fast-wave simulations in acoustics, computational optimization, and 3D fabrication, our method is low-cost, adapts to different wireless routers and physical environments, and has a far-reaching impact by interweaving computational techniques to solve key problems in wireless communication.

## Categories and Subject Descriptors

C.2.1 [Computer-Communication Networks]: Network Architecture and Design—*Wireless communication*

## Keywords

Wireless networking; 3D fabrication; Signal map; Design

## 1. INTRODUCTION

Today most Wi-Fi access points (APs) are omni-directional sources of electromagnetic waves. Since wireless channel is a broadcast medium, wireless transmissions suffer two well-known concerns. *First*, wireless performance degrades when multiple Wi-Fi APs transmit in an uncoordinated manner and the wireless signals interfere

with one another. *Second*, wireless transmissions are vulnerable to traffic eavesdropping and other security and privacy attacks. A third-party in a region where the signal strength is sufficiently strong can eavesdrop on transmitted data. Even if the wireless network is encrypted, the third-party can still obtain network information (e.g., channel number, received signal strength), and use the information to physically locate the AP or launch denial of service attacks.

Addressing both concerns requires judicious control over how wireless signals propagate in an environment. Specifically, we aim to strengthen the signal in regions where high performance is desired, and weaken the signal in regions where malicious third-parties could potentially be eavesdropping. This level of customization also allows network managers to plan the coverage regions of multiple APs to avoid harmful interference. It is an inherently challenging task given the complex nature of electromagnetic wave propagation and its interaction with the environment [5]. The common solution today is directional antennas, which concentrate wireless signals in a desired direction using either horn-shaped antennas or an array of antenna elements with phases electronically configurable. However, directional antennas dictate limited working scenarios. They can be made in a small form-factor for high-frequency band (e.g., 60GHz) transmissions because of the short signal wavelength. Unfortunately, for lower frequency bands such as Wi-Fi bands (2.4 or 5GHz), directional antennas are typically bulky, expensive, do not come with ordinary routers by default, and have very limited granularity and flexibility in controlling signal propagation in a practical environment. It is hard, if not impossible, to control wireless signal coverage in a fine granularity while taking into account a specific wireless propagation environment.

In this paper, we propose WiPrint, an interdisciplinary approach to direct wireless signals and customize the resulting signal strength distribution in the 3D space. Our approach integrates wireless communication, computational optimization, and 3D fabrication. The key idea is to place a glossy reflector surrounding a wireless AP. The reflector shape is computationally optimized such that it steers the wireless signals to form a desired strength distribution. In fact, anecdotal experiments [4] have demonstrated substantial bandwidth gain by simply placing a soda can behind a Wi-Fi AP.

Permission to make digital or hard copies of all or part of this work for personal or classroom use is granted without fee provided that copies are not made or distributed for profit or commercial advantage and that copies bear this notice and the full citation on the first page. Copyrights for components of this work owned by others than ACM must be honored. Abstracting with credit is permitted. To copy otherwise, or republish, to post on servers or to redistribute to lists, requires prior specific permission and/or a fee. Request permissions from [Permissions@acm.org](mailto:Permissions@acm.org).

*HotWireless '15*, September 11, 2015, Paris, France.

© 2015 ACM. ISBN 978-1-4503-3699-4/15/09 ...\$15.00.

DOI: <http://dx.doi.org/10.1145/2799650.2799653>.

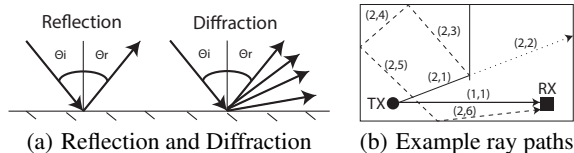


Figure 2: Ray tracing.

WiPrint generalizes the idea of reflecting wireless signals in two aspects: (i) WiPrint aims to achieve *any* user-specified target signal distribution by optimizing the fine detail of the reflector shape, and (ii) our optimization considers the wireless signal’s interaction with a specific environment and thus can adapt to different environmental settings. Our approach echoes the principle of caustic design in computer graphics [17], which creates a physical object to refract light rays such that the transmitted rays form a desired caustic image on the receiving screen. In a similar sense, we create an object (the reflector) that attenuates radio waves to form a signal “caustic pattern” (signal map). Our approach differs from MIMO algorithms used in phased antenna arrays in that it controls the signal at a much finer level of granularity.

Specifically, as shown in Figure 1, WiPrint takes the following input: (i) a digitalized environmental setting (e.g., furniture, floor plan) obtained using 3D geometry reconstruction techniques [7, 12], which have been well developed in computer vision and graphics; and (ii) the desired wireless coverage, which can be a user-specified Wi-Fi signal heatmap, or a set of small coverage regions selected by the user, or an ideal Wi-Fi signal distribution automatically learned based on users’ mobility pattern and density. The core of our approach is a computational algorithm that optimizes reflector shape to form the desired signal distribution. Finally, we use commodity 3D printers to fabricate the optimized reflector and mount it near the wireless router to physically realize the desired signal distribution. WiPrint is low-cost, easy-to-use by ordinary users, requires no modification of existing wireless APs, and adapts to varying physical environments and a wide range of frequency bands.

## 2. WIRELESS PROPAGATION MODEL

The first core component of WiPrint is a model of wireless signal propagation, which predicts the wireless signal distribution in a given environment and in turn helps to design the reflector shape. Given the rich literature, we start with examining the representative models ranging from the simple uniform pathloss model [10] to sophisticated models such as empirical models for indoor signal propagation (ITU model [8]) and ray-tracing models [20]. Ultimately we chose a 2D ray tracer with a partition model [6, 13], which is a good simulation of wireless propagation in a typical indoor environment. We extend conventional ray tracing with the Uniform Theory of Diffraction (UTD) [19] in acoustics to capture signal diffraction.

**Ray Tracing.** Ray tracing [20] captures the wave behavior of wireless radio waves using rays exhibiting particle-like behavior. It has been widely used by prior studies [9, 11, 13] as one of the most accurate propagation models with tractable complexity. Given a transmitter, wireless signals are represented by rays launched from the transmitter. Rays are attenuated around the room until they reach a receiver. The received signal strength (RSS) of a ray at the receiver is determined by the distance traveled by the ray, the ray’s frequency and the number of reflections and transmissions it encountered before reaching the receiver. We will discuss our propagation model for each ray in the later section.

We consider the *reflection* and *diffraction* of the radio rays when they propagate in an environment with surrounding objects (e.g., walls, furniture). Other wave phenomena like scattering are not modeled since they are difficult to simulate [18] and have negligible impact on the resulting signal map [13]. For signal reflection, we focus on specular reflection (Figure 2(a)). Furthermore, inspired by the fast-wave acoustics simulations in computer graphics, we leverage the Uniform Theory of Diffraction (UTD) [19] in acoustics simulations to capture the diffraction of wireless signals.

Figure 2(b) shows different types of attenuation handled by the ray tracer and how rays are decomposed to take care of them. Each ray segment is denoted by the tuple  $(i, j)$  where  $i$  is the ray number and  $j$  is the segment number of that ray. When multiple rays reach a receiver, we sum up all rays’ RSS values in mW.

**Propagation Model of a Single Ray.** To model the signal attenuation of a single radio ray, we apply the partition model [6, 13], which extends the uniform pathloss model by taking into account different signal attenuation caused by various objects (e.g., walls, floors, ceiling, furniture).

In particular, let  $PL_i$  denote the pathloss in dBm at location  $i$ .  $PL_i$  is calculated as below:

$$PL_i = PL_0 + 10\alpha \log_{10}(d_i) + \beta N_{ref} + \gamma N_{trans} + \theta N_{diff}, \quad (1)$$

where  $PL_0$  is the reference pathloss value measured in advance,  $\alpha$  is the pathloss exponent,  $d_i$  is the distance that the ray has traveled,  $N_{ref}$ ,  $N_{trans}$ , and  $N_{diff}$  are the number of reflections, transmissions, and diffractions, and  $\beta$ ,  $\gamma$ , and  $\theta$  are the corresponding coefficient respectively. To calibrate the parameters  $(PL_0, \beta, \gamma, \theta)$  in the above equations, we apply simulated annealing [13], a randomized algorithm, to seek the parameter values that minimize the root mean square error (RMSE) of the RSS estimation. To calibrate these parameters, we only need measurements at a small number of sampled locations, rather than a complete site survey. Thus our model can easily adapt to varying environments. We set the maximum number of rays to be 500 and the threshold for the maximum number of reflections, transmissions, and diffractions to be 2. As our propagation models are currently 2D, WiPrint outputs an estimated signal map within 500 ms.

While we use the above models in our current design, WiPrint framework is general and can be integrated with other propagation models. We also plan to extend our 2D signal propagation model to the 3D space by incorporating the signal’s interaction in the 3D environment (Section 6). Helmholtz equations are often used to visualize Wi-Fi signal maps in a 3D environment as waves [1]. This model, however, entails a significantly higher computational complexity and can take minutes [1] to generate a complete signal map. We plan to examine alternative solutions with lower complexity.

## 3. COMPUTING THE REFLECTOR SHAPE

The second core component of WiPrint is the algorithm to compute a detailed reflector shape that achieves a desired signal distribution. The computational algorithm takes the following input: 1) the user’s desired signal map  $M_D$  that is either *low-resolution* or *high-resolution*. A low-resolution map means that the user roughly specifies regions where they desire stronger or weaker signals. Figure 1 shows an example of the low-resolution desired signal map, where red and black regions denote areas where users desire stronger or weaker (or no) signals respectively. A high-resolution signal map divides the environment into small cells and marks a target RSS value for each cell; 2) the environment layout  $E$ ; 3) the AP location  $L_{AP}$ ; and 4) the initial reflector shape  $R$  represented by a set of features.

---

**Algorithm 1** Simulated Annealing

---

```
1:  $T_{max} \leftarrow 1000$ 
2:  $T \leftarrow T_{max}$ 
3:  $T_{min} \leftarrow 0.001$ 
4:  $coolingRate \leftarrow 0.99$ 
5: initialize  $R$ 
6:  $M_R \leftarrow genSignalMap(E, L_{AP}, R)$ 
7:  $f \leftarrow \delta(M_D, M_R)$ 
8: while  $T > T_{min}$  do
9:    $R' \leftarrow mutate(R)$ 
10:   $M_{R'} \leftarrow genSignalMap(E, L_{AP}, R')$ 
11:   $f' \leftarrow \delta(M_D, M_{R'})$ 
12:   $p \leftarrow e^{\frac{f'-f}{T}}$ 
13:  if  $f' \geq f$  or  $rand[0, 1] \leq p$  then
14:     $f \leftarrow f'$ 
15:     $R \leftarrow R'$ 
16:  end if
17:   $T \leftarrow T \cdot coolingRate$ 
18: end while
19:  $R^* \leftarrow R$ 
```

---

Our algorithm iteratively mutates the initial reflector shape, estimates the resulting signal strength distribution map  $M_R$  for the mutated shape  $R$ , calculates the difference between desired and estimated signal maps, and searches for the optimal shape  $R^*$  that minimizes the difference. Next we describe the key steps in detail.

**Defining the Reflector Shape.** We define the reflector shape as a contiguous series of lines. In this preliminary work, we explore reflectors that can be represented as a polynomial function. The polynomial is defined by its degree and the location of its control points relative to the AP. We represent the reflector as a set of curves and use Lagrange polynomials to interpolate its shape at control points. The reflector shape  $R$  is a feature vector denoting the properties of a polynomial function.

**Searching for the Optimal Reflector Shape.** Our searching algorithm initializes the reflector shape  $R$  as a straight horizontal line above the AP. It then mutates the shape over iterations. To evaluate the effectiveness of a mutated shape  $R$ , we calculate the difference  $\delta(M_D, M_R)$  between the desired signal map  $M_D$  and the signal map  $M_R$  generated by placing the reflector  $R$ . For high-resolution input signal maps,  $\delta(M_D, M_R)$  is calculated as below:

$$\delta(M_D, M_R) = - \sum_{i=0}^n |M_D(i) - M_R(i)|,$$

where  $n$  denotes the number of cells in the signal maps,  $M_D(i)$  and  $M_R(i)$  are the signal strength values in dBm at cell  $i$  in the desired and estimated map respectively. For low-resolution maps,  $M_D$  consists of a set of good regions  $A_{good}$ , where users desire strong wireless signals, and bad regions  $A_{bad}$ , where users desire no or weak signals. Then  $\delta(M_D, M_R)$  is calculated as below:

$$\delta(M_D, M_R) = \sum_{i \in A_{good}} (M_R(i) - S_{min}) + \sum_{i \in A_{bad}} (S_{max} - M_R(i)),$$

where  $S_{min}$  and  $S_{max}$  are the signal value thresholds for good or bad signal regions.

Given the objective function, we apply simulated annealing, a randomized optimization algorithm, to search for  $R^*$ :

$$R^* = \underset{R}{\operatorname{argmax}} \delta(M_D, M_R).$$

In a nutshell, the algorithm greedily maximizes the objective function while avoiding being stuck at local optimums. Simulated annealing combines hill-climbing and exploration to search for  $R^*$ .



(a) Concave reflector (b) Partial square-wave reflector (c) Square-wave reflector with a metal layer

**Figure 3: Reflectors in experiments.**

Hill-climbing greedily maximizes the objective function, i.e., accepts a candidate shape only if it is strictly better than the previous solution. The exploration part of the algorithm accepts candidate solutions with objective function values lower than the previous solution, with an acceptance probability of  $p$  [13]. Algorithm 3 lists the detail. Although simulated annealing often needs to test a fairly large number of candidate solutions to arrive at a global optimum, it is a reasonable solution in our current 2D simulator. We plan to explore more advanced and efficient search algorithms such as the optimal transport algorithm in [17], once we progress to 3D propagation models.

**Fabricating the Reflector.** The final step of WiPrint is to fabricate the reflector in the optimized shape. The ideal materials of the reflectors are glossy metals like aluminum, since they absorb less electromagnetic waves and better reflect wireless signals with small energy loss. To maintain a low cost, we first 3D print a plastic reflector substrate and then coat it with a thin metal layer [21] or wrap it tightly with aluminum sheets (Figure 3(b,c)).

## 4. FEASIBILITY RESULTS

We examine the feasibility of WiPrint using an off-the-shelf Wi-Fi router and 3D-printed reflectors. We seek to understand the accuracy of our signal propagation model, the impact of the reflectors on the resulting signal distribution, the effectiveness of the optimized reflector shape, and WiPrint's cost compared to directional antennas.

**Measurement Setup.** We conduct experiments in a large indoor space 25.2 m  $\times$  14.4 m in size. We partition the space into 18  $\times$  18 cells. Our Wi-Fi transmitter is a Linksys WRT54GL wireless router with two external antennas operating on the 2.4 GHz frequency band. The router's power is set to a low power of 1mW to yield quicker signal degradation and a higher-contrast signal map. We also set the router's operating channel to the least congested channel to minimize interference from other Wi-Fi links. The receiver is a MacBook Pro. We place the receiver in the center of each cell, capture router's beacons for 45 seconds, and average the RSS values in received beacons as the RSS value at this cell. Manually measuring all the cells in the room currently takes 4-5 hours.

**Accuracy of Signal Propagation Modeling.** We first examine how accurately our signal propagation model can match the actual signal propagation. We start with the baseline scenario where no reflector is placed around the transmitter. We measure the signal maps when placing the AP in the center or in the corner of the room, and examine how close they are to the signal maps estimated by the propagation model.

Figure 4(a,b) show that the estimated signal maps closely match the actual maps. We further plot the CDF of the estimation error of each cell's RSS value, and compare our chosen model (ray tracing) to other representative models (uniform pathloss and ITU models). Overall, ray tracing model significantly outperforms other models and controls the maximal estimation error within 4 dBm in both scenarios. Adding the signal diffraction model further reduces

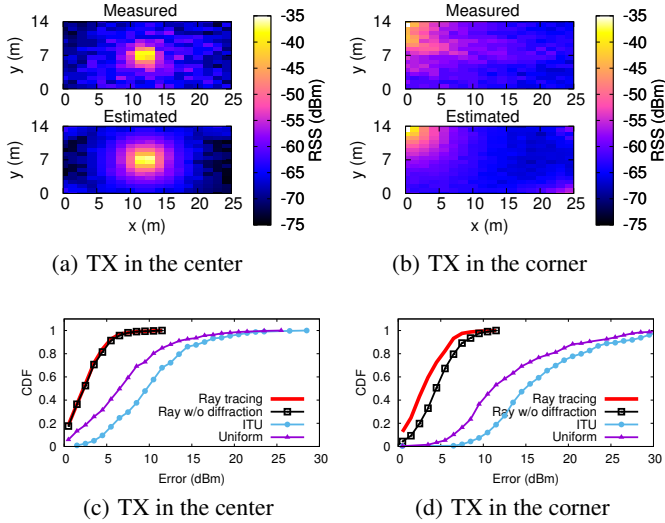


**Figure 4:** When no reflector is placed around the transmitter, (a,b) compare the measured and estimated signal maps, and (c,d) show the CDFs of estimation errors.

the estimation error by a small margin when the transmitter is in the corner. This is because the AP is closer to the environment’s boundaries, causing many rays to be reflected early along its path and combined through multi-path propagation. The diffraction model simulates the build-up of scattered rays in the corner.

**Impact of Reflector Shape.** Next we examine the impact of reflector shape on the resulting signal distribution. We test two types of reflector shapes: concave and square-wave reflector. Figure 3(c) shows half of the square-wave reflector that we have printed. We use foil tape to attach reflector parts together. For both reflectors, we apply foil tape on the reflector surface. Figure 3(a,c) show their final looks and their sizes with respect to the router.

Figure 5 compares the measured and estimated signal maps when placing reflector around the AP. Overall the results are promising. We observe that the concave reflector effectively directs the signal to the south of the room as expected. The resulting measured signal map matches the estimated signal map. In comparison, the square-wave reflector leads to a larger discrepancy between the measured and estimated maps. We observe signal leakage in the east and west of the room, indicating that the reflector does not completely block the Wi-Fi signals in these two directions. We plan to test more types of metal layer with different thickness and better coating to understand the impact of the reflector material. We also plan to examine a greater variety of reflector shapes to understand the level of control granularity made possible by fabricated reflectors.

**Effectiveness of Optimized Reflector Shape.** We now examine the effectiveness of our optimized reflector shape on steering wireless signal propagation to form the desired signal coverage distribution. Figure 1 shows an example low-resolution desired signal map on the bottom left, the optimized reflector shape calculated by WiPrint algorithm, and the estimated signal map after placing the reflector behind the AP. Figure 6 shows another example where users desire stronger signals in region 2 and 3 while weaker or no signals in region 1 and 4. Using the optimized reflector shape (Figure 6(b)) generated by WiPrint, we effectively steer the signals away from region 1 and 4 and strengthen the signal in region 2 and 3, where the signal was originally weakened by the wall blockage. Overall in both examples, the resulting signal maps match the target signal

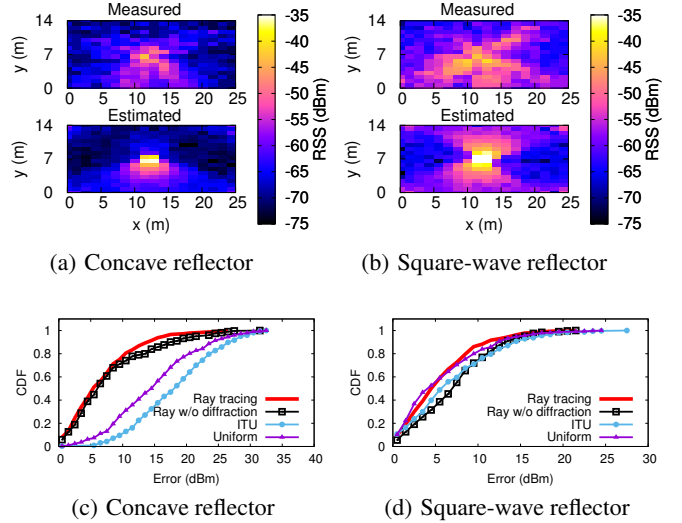


**Figure 5:** Impact of the reflector shape on the resulting signal distribution. (a,b) compare the measured and estimate signal maps and (c,d) shows the CDFs of estimation errors.

maps, demonstrating the efficacy of WiPrint’s preliminary algorithm design. For the future work, we plan to evaluate desired signal maps (both in low and high resolution) more extensively, 3D fabricate the optimized reflector shape, and measure the actual signal maps.

**Cost Analysis.** Printing both parts of the square-wave reflector took roughly 17 hours and consumed 6 in<sup>3</sup> of material for the model and 3 in<sup>3</sup> of material for support purposes. The material used by the printer was ABS-P430 thermoplastic and the material of the reflector costs around \$45. This is significantly cheaper than directional antennas (e.g., the Phocus Array used in [15, 18] costs \$9000 [2]). Less advanced directional antennas cost around \$100 [3]. This low cost makes our solution accessible to a wide-range of consumers, who can easily use online 3D printing services to manufacture the reflector, even if they do not have physical access to a 3D printer.

## 5. RELATED WORK

**Optimizing Wireless Coverage.** Prior work has studied optimizing the AP placement to maximize the signal strength in certain areas [16]. However, moving the AP to improve the strength in one area would also result in the decline of signal strength in another area. Thus, such methods can not create multiple maximums. Changing the AP location is also a coarse-grained solution without any control on the exact boundaries of the signal propagation. In [18], Sheth *et al* used multiple directional APs to create a desired wireless coverage shape. As the authors have noted, directional antennas lose their directionality when being applied to indoor settings because of the multi-path effects. WiPrint differs in that it customizes the wireless signal coverage using only a single AP without expensive directional antennas, adapts to different environment, and achieves fine-grained control of the coverage shape.

**Caustic Design in Computer Graphics.** We are inspired by caustic design in computer graphics, which creates a physical object to refract light rays and form a desired image on a screen [17]. Their work uses an advanced 3D optimization method to transform an unperturbed pattern of light to a desired light pattern. However, we rely on a simpler model widely used and tested in the field of wireless networking. The refractive object must be constructed to a high degree of precision. However, for our system the level

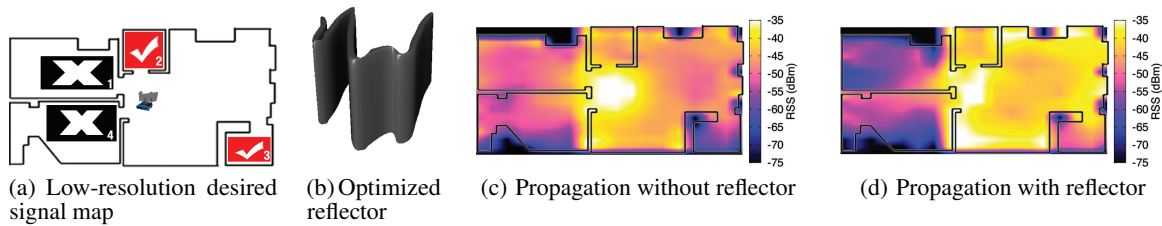


Figure 6: Effectiveness of optimized reflector shape in steering wireless signal propagation.

of variance for wireless propagation is high, therefore a relatively simple solver using Monte Carlo method would suffice [17].

## 6. CONCLUSION AND FUTURE WORK

We presented WiPrint, an interdisciplinary approach that steers wireless signal propagation to form a desired signal distribution in the space. WiPrint directs wireless signals using a glossy reflector surrounding the wireless AP. WiPrint judiciously calculates the fine detail of the reflector shape by leveraging recent advances in 3D fabrication, computational optimization, and computer graphics. Fine-grained control of the wireless propagation has a far-reaching impact on the energy efficiency, security, and performance aspects of wireless communication.

We also recognize the limitations of our preliminary study and plan to work on the following additional challenges and extensions:

**3D Propagation Modeling.** WiPrint is currently based on 2D models of the environmental setup and signal propagation. We plan to examine modeling the signal propagation in 3D. We can leverage 3D geometry reconstruction techniques in computer graphics to digitize 3D environments for simulating wireless propagation and enhance our current propagation model to incorporate the signal's interactions in 3D. This will allow us to take into account the height of the AP, and the height of any partitions or obstructions in the environment. We will also explore the use of robots (e.g., Roomba) to automate detailed signal measurements [14].

**Multiple Reflectors.** Our current algorithm focuses on generating a single reflector in the optimized shape. An interesting extension is to consider multiple reflectors that can relay wireless signals to regions unreachable due to severe occlusion. Multiple reflectors can also help form more complicated desired signal distribution in a complex environment.

**Higher Frequency Bands.** We plan to extend WiPrint to higher electromagnetic wave frequency bands such as millimeter-wave band and visible light spectrum band. Electromagnetic waves at higher frequency have better reflection properties and thus can be more effectively directed by reflectors. In addition, the reflector can be made in smaller size because of the shorter wave length. As a result, one can potentially integrate the optimized reflectors inside the radio by placing them close to the radio antenna.

**Quantifying Granularity.** We plan to quantify the level of granularity that WiPrint provides using 3D printed reflectors. As the basis of WiPrint's fine-grained control, the printing resolution is already 0.1 mm for consumer-level 3D printers (e.g., MakerBot) and 0.01 mm for higher-end printers. We will also compare WiPrint to the MIMO algorithms used in phased antenna arrays.

## 7. ACKNOWLEDGMENTS

We thank anonymous reviewers and Jiawen Chen (Google) for the constructive comments. This work is supported in part by the

Dartmouth Burke Research Initiation Award and the Class of 1993 Alumni Fund at Dartmouth College, the National Science Foundation (CAREER-1453101) as well as generous gifts from Intel. Any opinions, findings, and conclusions or recommendations expressed in this material are those of the authors and do not necessarily reflect those of the funding agencies or others.

## 8. REFERENCES

- [1] <http://jasmcole.com/2014/08/25/helmhurts/>.
- [2] <http://www.tmcnet.com/usubmit/2008/01/24/3227843.htm>.
- [3] <http://www.radiolabs.com/products/wireless/directional-wireless-antenna.php>.
- [4] Dramatically Improve WIFI Speed With a Soda Can! <https://youtu.be/yz4aPaebe-k>.
- [5] ANDERSEN, J. B., RAPPAPORT, T. S., AND YOSHIDA, S. Propagation measurements and models for wireless communications channels. *Communications Magazine, IEEE* 33, 1 (1995), 42–49.
- [6] BAHL, P., AND PADMANABHAN, V. N. RADAR: An in-building RF-based user location and tracking system. In *Proc. of INFOCOM* (2000).
- [7] CHEN, J., BAUTEMBACH, D., AND IZADI, S. Scalable real-time volumetric surface reconstruction. In *Proc. of SIGGRAPH* (2013).
- [8] CHRYSIKOS, T., GEORGOPOULOS, G., AND KOTSOPOULOS, S. Site-specific validation of ITU indoor path loss model at 2.4 GHz. In *Proc. of WoWMoM* (2009).
- [9] GERMAN, G., ET AL. Wireless indoor channel modeling: statistical agreement of ray tracing simulations and channel sounding measurements. In *Proc. of ICASSP* (2001).
- [10] GOLDSMITH, A. *Wireless communications*. Cambridge Univ Pr.
- [11] ISKANDER, M. F., AND YUN, Z. Propagation prediction models for wireless communication systems. *Microwave Theory and Techniques, IEEE Transactions on* 50, 3 (2002), 662–673.
- [12] IZADI, S., ET AL. KinectFusion: Real-time 3D Reconstruction and Interaction Using a Moving Depth Camera. In *Proc. of UIST* (2011).
- [13] JI, Y., BIAZ, S., PANDEY, S., AND AGRAWAL, P. ARIADNE: a dynamic indoor signal map construction and localization system. In *Proc. of MobiSys* (2006).
- [14] KIM, K.-H., MIN, A. W., AND SHIN, K. G. Sybot: an adaptive and mobile spectrum survey system for wifi networks. In *Proc. of MobiCom* (2010).
- [15] NAVDA, V., ET AL. MobiSteer: using steerable beam directional antenna for vehicular network access. In *Proc. of MobiSys* (2007).
- [16] PANJWANI, M. A., ABBOTT, A. L., AND RAPPAPORT, T. S. Interactive computation of coverage regions for wireless communication in multifloored indoor environments. *Selected Areas in Communications, IEEE Journal on* 14, 3 (1996), 420–430.
- [17] SCHWARTZBURG, Y., ET AL. High-contrast computational caustic design. *ACM Transactions on Graphics (TOG)* 33, 4 (2014), 74.
- [18] SHETH, A., SESHAN, S., AND WETHERALL, D. Geo-fencing: Confining Wi-Fi coverage to physical boundaries. In *Pervasive Computing*. Springer, 2009, pp. 274–290.
- [19] TSINGOS, N., ET AL. Modeling acoustics in virtual environments using the uniform theory of diffraction. In *Proc. of SIGGRAPH* (2001).
- [20] VALENZUELA, R. A. A ray tracing approach to predicting indoor wireless transmission. In *Proc. of VTC* (1993).
- [21] ZHANG, Y., YIN, C., ZHENG, C., AND ZHOU, K. Computational hydrographic printing. *Proc. of SIGGRAPH* (2015).